Available online at www.sciencedirect.com
ScienceDirect
Applied Acoustics 68 (2007) 281–295
applied acoustics
www.elsevier.com/locate/apacoust

Developments in active noise control sound systems for magnetic resonance imaging

John Chambers [a], Dave Bullock [a], Yuvi Kahana [b], Alexander Kots [b], Alan Palmer [a,*]

[a] *MRC Institute of Hearing Research, University Park, Nottingham NG7 2RD, UK*
[b] *Phone-Or Ltd., 17 Hatasia Street, Or-Yehuda 60212, Israel*

Received 12 April 2005; received in revised form 4 October 2005; accepted 5 October 2005
Available online 8 May 2006

Abstract

Magnetic resonance imaging (MRI) scanners can produce noise measuring over 130 dB SPL. This noise stimulates the auditory nervous system, limiting the dynamic range for stimulus driven activity in functional MRI (fMRI) experiments and can influence other brain functions. Even for structural scans it causes subject anxiety and discomfort in addition to the impediment to communications. Here we describe the realization and validation of a sound system for sound presentation inside an MRI scanner and the modifications to a standard active noise control technique for use in the noisy and compact environment of the scanner. This paper provides a review of the technology available for the presentation of audio stimuli in an MRI environment and the modifications required for the active control of scanner noise. Some of the content has been previously published [Chambers J, Akeroyd MA, Summerfield AQ, Palmer AR. Active control of the volume acquisition noise in functional magnetic resonance imaging: method and psychoacoustical evaluation. J Acoust Soc Am 2001;110(6):3041–54; Levitt H. Transformed up–down methods in psychoacoustics. J Acoust Soc Am 1971;49:467–77], but this paper goes further in describing the stages of development as the system performance was optimised. The performance of the system and both the objective and subjective reduction of the scanner noise are reported. Finally, we discuss recent improvements to the system that are currently being evaluated and describe the theory of opto-acoustical transducers that operate on the principle of light

* Corresponding author.
E-mail address: alan@ihr.mrc.ac.uk (A. Palmer).

0003-682X/$ - see front matter
doi:10.1016/j.apacoust.2005.10.008

modulation. These are immune from, and do not create, electro-magnetic interference (EMI) and radio-frequency interference (RFI).

Keywords: Active noise control; Magnetic resonance imaging; fMRI; Opto-acoustic transducers

1. MRI noise characteristics and effects

MRI imaging has been increasingly used for both medical diagnoses and for research purposes over the last 10 years. Clinically, MRI is used to produce anatomical images of soft tissue without exposing subjects to harmful radiation. For this purpose, the MRI scanner runs a "Structural" scan sequence in order to produce a high resolution image that is built up over a period of minutes. MRI scanning is also used in research studying "functional" activation of the brain by taking a low resolution image of the whole brain very rapidly. Oxy- and deoxy-haemoglobin have different magnetic properties that allow the MRI scanner to detect areas of the brain that are active during particular tasks by the increased blood flow to those areas. By subtracting images of the brain taken at rest from those taken during a task, the areas involved during that task are highlighted. A main problem of MRI is however, the high levels of sound that the scanning process generates. Magnetic resonance imaging (MRI) scanners can produce noise measuring over 130 dB SPL (see [1]). This noise stimulates the auditory nervous system, limiting the dynamic range for stimulus driven activity in functional MRI (fMRI) experiments and can influence other brain functions [2–13]. Even for structural scans it causes subject anxiety and discomfort in addition to the impediment to communications. The spectra of the sounds generated during functional scans and during structural scans are markedly different. fMRI typically uses echo planar imaging (EPI) sequences that produce sounds with spectra with a sharp peak at a frequency typically between 500 Hz and 3 kHz (different for different scanners and sequences) that repeat over a matter of seconds. Structural sequences produce a more dispersed sound spectrum with most of the energy at low frequencies which can change slowly over a matter of minutes. The functional EPI scanner noise is usually louder than the structural noise. Fig. 1 shows the spectra of the sounds recorded during sample EPI and structural scans.

2. Sound system requirements and restrictions of the MRI environment

The sound system was designed for the presentation of high quality sounds to subjects taking part in auditory fMRI studies. Due to the nature of the experiments, the sound system was required to have a wide bandwidth (0.1–20 kHz), a high output level (100 dB SPL over the entire bandwidth) and a flat frequency response. The MRI environment imposes some severe constraints on the materials that can be used in close proximity to the subject in the scanner. The presence of metal (either ferrous or non-ferrous) distorts the MRI image and shields the head from the radio signal that the scanner uses to create the image. Any radio-frequency noise created by the sound system will appear as noise or lines in the scanner image. Additionally, the scanner produces high-intensity radio-frequency pulses that will induce voltages in any conductors inside the scanner. Finally, the head-coil that picks up the signal from the subject's body needs to be as close to the head as possible to maximised the received signal, leaving very little space between the subject's ears and the scanner coil.

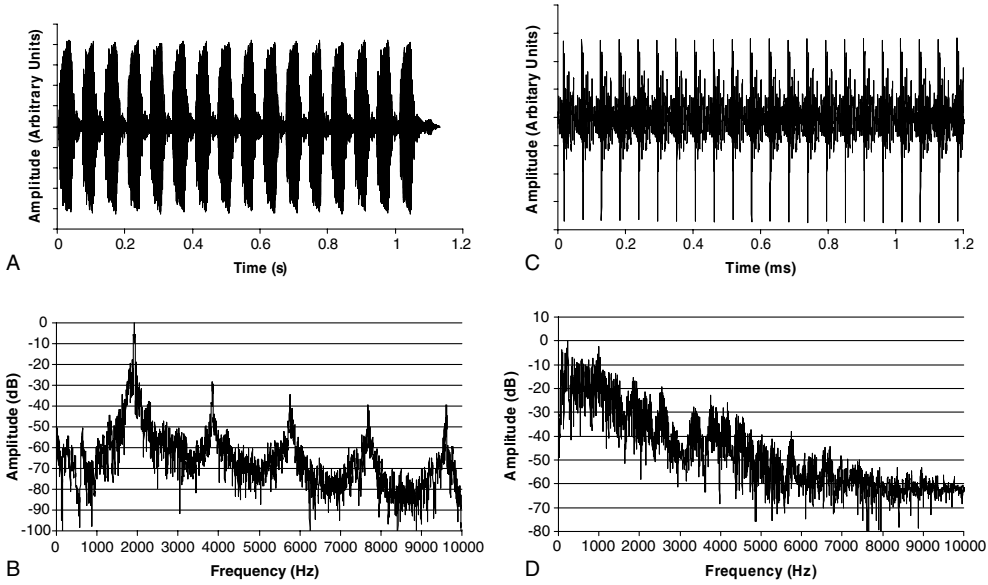

Fig. 1. Waveforms and spectra of MRI scanner generated sounds. (A) Waveform of a 16-slice volume acquisition sequence using echo planar imaging at 3 T. (B) Spectrum of the scanner sound in A showing the fundamental component at 1900 Hz with higher frequency harmonically related components. (C) Waveform of a structural sequence and (D) the spectrum of the structural sequence showing a low pass noise spectrum. A and B adapted from [24] with permission.

3. First prototype MRI sound system

Two different sound transducers were considered suitable for use in an MRI scanner; electrostatic or piezoelectric. Electrostatic headphones were used as they were available commercially (Sennheiser HE60/HEV70; now discontinued) with a performance exceeding the required acoustic specification. The metal content of the electrostatic transducers was minimal and, due to the high impedance of electrostatic diaphragms, the connections to the transducers could be carbon fibre rather than copper. In order to protect the subject from the intense sound, the sound system headset was housed in a set of Bilsom ear defenders as shown in Fig. 2. Performance testing was done using a KEMAR (Knowles Electronics Mannequin for Acoustic Research) mannequin with small pinna and a Brüel & Kjäer 12.5 mm condenser microphone in a Zwislocki coupler. To evaluate the effect of building the electrostatics into the ear defenders, wideband noise was presented through both the unmodified Sennheiser HE60/HEV70 headphones and then through the sound system headset. The spectra were measured from the KEMAR microphone. To test the efficacy of the ear defenders, wideband noise was presented from a speaker pointing at the KEMAR ear. The level of sound recorded by the microphone with the sound system headset and with unmodified Bilsom ear defenders was recorded. Fig. 3 shows the results of these measurements, which confirmed that the frequency response was not compromised and the attenuation characteristics of the ear defenders were adequately maintained.

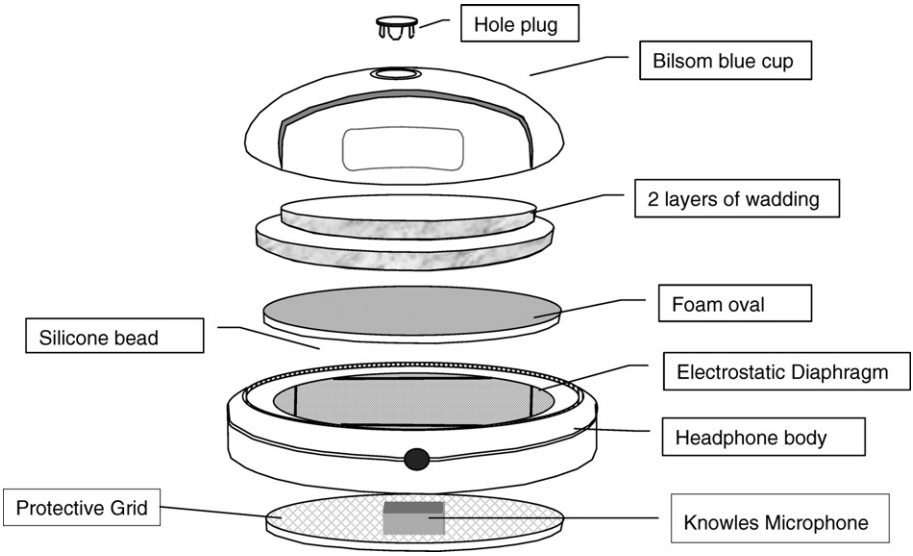

Fig. 2. Construction details of the incorporation of the electrostatic transducer and error microphone into the Bilsom ear defender.

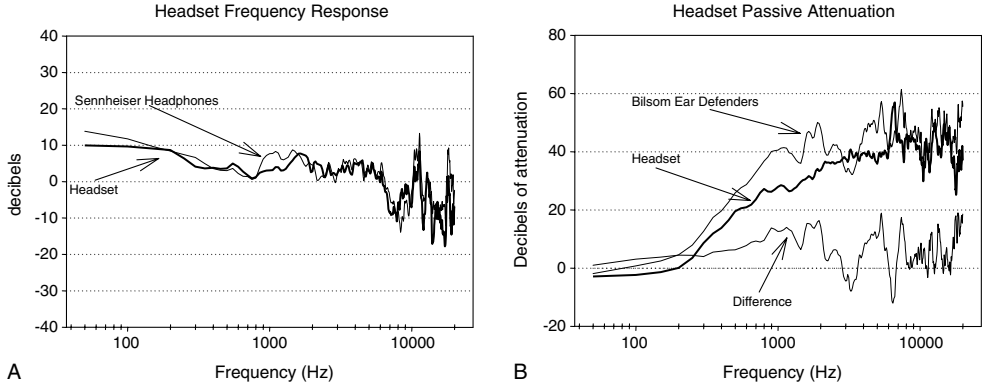

Fig. 3. (A) The frequency response of the electrostatic earphones measured using a KEMAR. The original phone is shown by the thin lines and the phone after incorporation in the ear defenders by the thick line. (B) The passive attenuation of the Bilsom ear defenders before (thin line) and after (thick line) incorporating the electrostatic transducers. The thin line at the bottom shows the difference.

4. Methods of reducing subjective MRI scanner noise

Several techniques are routinely employed to actually reduce the background noise and scanner noise or to minimise its effect. These measures have been mostly passive. They include earplugs, ear defenders, lining the scanner bore with sound-absorbing foam and making measurement in time epochs unaffected by the scanner noise [4,9,12–15]. However, since it is difficult to achieve more than 40 dB of attenuation with these methods [16–18], the scanner noise can still reach levels of 70–90 dB SPL at the listeners' ears. The passive

attenuation that can be achieved by ear defenders is limited by the dimensions of the ear-cups with slimmer designs generally achieving less attenuation at lower frequencies.

Further attenuation of the airborne sound can be achieved by active noise control. The principle is simply to create a control sound that interferes destructively with the incident scanner sound at the listener's ear. In principle, the control loudspeaker can either be mounted within a headphone to give local cancellation or it can be mounted remote from the subjects head and used to create a ''quite zone'' around the subject's ear. Any sound delivery system for auditory fMRI that includes active noise control is required to allow presentation of sound to the subject, whilst removing or reducing the MRI scanner noise.

There are two main topologies for active noise control; feed-forward and feed-back. The feed-back topology uses a microphone placed close to the point where reduction is required to sample the sound propagating towards the subject. This provides a reference signal that is filtered and used to drive a loudspeaker. The loudspeaker generates a control sound that propagates to the subject and destructively interferes with the incident sound, reducing its level. The time required for the control signal to propagate from the loudspeaker to the subject, and the necessity for maintaining stability at all frequencies, means that the upper frequency of control for feed-back systems is commonly limited to a few hundred Hertz. This limit is significantly below that required for fMRI, as significant acoustic energy generated by an EPI sequence can be found at frequencies as high as 3–4 kHz (Fig. 1). Furthermore, there is only one input to a feed-back system: a microphone placed close to the ear. This microphone would pick up both the scanner sound and the sounds being deliberately presented to the subject, and so the noise control system would attempt to cancel both. For these reasons, feed-back control can only usefully be used for low-frequency structural MRI noise.

The feed-forward topology uses a reference microphone placed close to the noise source to capture the noise that is propagating towards the noise-control point. A processor takes this ''advanced'' noise and filters it so that when presented through the control loudspeaker, noise-reduction is achieved. An ''error'' microphone, the placement of which defines the point of control (the ''monitoring point''), is placed close to the listener's ear and provides an electrical copy of the residual noise. This topology is more suitable than the feed-back topology for application in fMRI for two reasons. First, the availability of the advanced reference signal allows the system to compensate for the delays introduced by the distance between the control loudspeaker and the error microphone. Thus, potentially, the maximum frequency can be extended sufficiently to reduce high-frequency EPI gradient noise. Second, because the reference signal contains only the noise, the system can attenuate the scanner sound while leaving the signals being presented to the subject intact.

5. Theory of noise control system operation

The noise control algorithm used is a variation of the single channel feed-forward filtered-x adaptive controller [19]. A block diagram of this standard implementation is shown in Fig. 4. Since the whole system is implemented digitally, the continuous signals are replaced by the sampled signals and designated by the sample number (n). Hence, the noise propagates along an acoustic path M and is represented as a sound $d(n)$ at the error microphone. A reference microphone close to the noise source generates a reference signal $x(n)$. This reference signal is processed by an adaptive filter (see below for details) and the output $y(n)$ drives a loudspeaker that produces a sound that propagates to the control point. The control point microphone samples the residual sound pressure giving

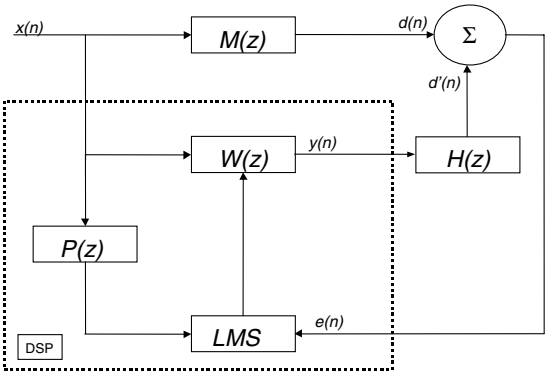

Fig. 4. A block diagram of the standard noise control topology (see text for details of the various paths and transfer functions marked) (from [24] with permission).

$e(n)$ which is the error between the noise sound and the cancellation control sound. This error signal is used by the adaptive filter algorithm to optimise the filter coefficients $W(z)$ to minimise the residual sound at the control point. The path from the loudspeaker to the control point has the transfer function $H(z)$. A digital filter model of this transfer function (or Plant) is included in the reference input to the adaptive filter in order to maintain stability. Thus both the reference input and error inputs to the update algorithm are processed through the same transfer function and the system remains stable at all frequencies.

Thus, as shown in Fig. 4, in a sampled system, we have: $M(z)$ the transfer function between the noise source and the error microphone (Primary path), $H(z)$ the transfer function between the control loudspeaker and the error microphone (Plant), $P(z)$ the electrical model of $H(z)$, $W(z)$ the adaptive filter, $x(n)$ the sampled noise signal, $y(n)$ the adaptive filter output and $e(n)$ the error microphone output.

6. Operation of the adaptive filter

The adaptive filter used a least mean squares (LMS) algorithm to iteratively adjust the coefficients of a finite impulse response filter using the error signal [20]. The error signal is first multiplied by a gain factor μ. The choice of the value for μ is critical; if it is too high the system becomes unstable whilst if μ is too low the system is slow to respond to changes. DC offsets in the analogue-to-digital converters and electronics can also cause instability: the plant has no response to DC so the adaptive filter will increase it's DC output until the dynamic range of the system is exceeded. This is prevented by multiplying each coefficient by just less than one ensuring that the coefficients tend towards zero over time. This is a standard technique in noise control [21] termed the leaky LMS algorithm.

The electrical model of the Plant impulse response is obtained using a maximum length sequence (MLS) analysis [22] that provides the linear part of the plant response ignoring non-linearities (see [23]).

7. Modifications to standard noise control for use in the MRI environment

Due to the very small distance of the sound generator from the subject's head in MRI the standard configuration cannot be used as the time delays are too small. There is a finite

time delay through the adaptive filter and anti-aliasing filters for the analogue-to-digital and digital-to-analogue converters used in the system. The control signal from the loudspeaker also takes time to propagate to the control point. Adding these times gives the minimum advance of the reference signal in order that the digital filter is causal. This time dictates the minimum separation between the reference microphone and the error microphone and in our system this is of the order of 17 cm [19]. Such a separation distance is not possible in the confined MRI environment. We therefore needed to obtain the reference signal from another source. The scan coils that create the MRI noise are crystal controlled and therefore highly stable in time over presentations. Thus we were able to record the signal from the error microphone during one EPI volume acquisition and use this recording as the reference during subsequent EPI presentations. This approach has two advantages. The first is that the scanner can trigger the output of the reference signal with as much time advance as required. Secondly, the reference signal is taken from the error microphone and has passed through the same acoustic path as the noise to be cancelled – indeed the reference signal is one exemplar of the noise that is to be cancelled.

The full system is shown in block diagram form in Fig. 5. The ability to play out the recorded reference before the acoustic signal is modelled using a negative time delay z^{+k}.

Letting $x'(n)$ be equal to the recorded reference then:

$$x'(n) = x(n)M(z) \tag{1}$$

the error microphone signal is the addition of the control signal and the noise:

$$e(n) = x(n)M(z) + x'(n)W(z)H(z)z^{+k} \tag{2}$$

If the adaptive filter converges perfectly $e(n) = 0$

$$x(n)M(z) = -x'(n)W(z)H(z)z^{+k} \tag{3}$$

Substituting $x'(n) = x(n)M(z)$

$$H(z)W(z)z^{+k} = -1 \tag{4}$$

$$W(z) = -(z^{+k})/H(z) \tag{5}$$

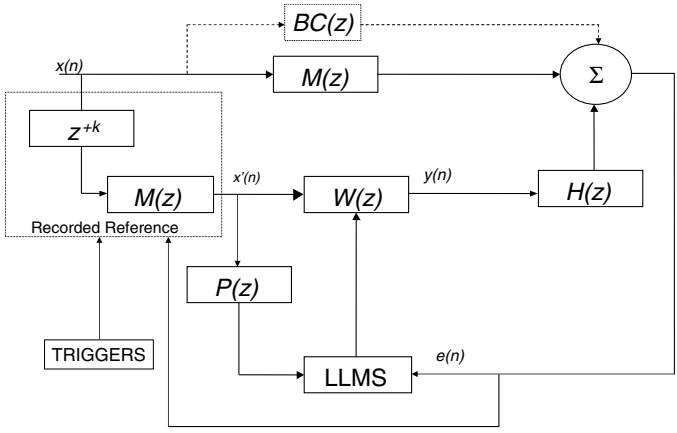

Fig. 5. A block diagram of the modified noise control topology necessary for use in MRI (modified after [27]). See text for details.

Thus the adaptive filter models the inverse of the plant together with an overall delay. There is no need to model the primary acoustic path in the adaptive filter as it is already present in the reference signal.

The major disadvantages of the recorded reference system are: (1) that it requires that the sound to be cancelled does not change radically in spectral content between presentations; (2) the reference signal must be captured before beginning cancellation; and (3) the onset of a trigger, the sound being generated and the cancellation sampling system must all start at the same time. Time variations lead to phase changes that increase with frequency. For example, to achieve a cancellation level of at least 25 dB up to 4 kHz the maximum time variation must be less than ± 2.2 μs. A 16 kHz sampling system (sampling interval of 62.5 μs) running continuously with triggers arriving asynchronously would have a peak time variation of ± 31.25 μs with a mean of ± 15.6 μs. Clearly, this time variation would severely limit the maximum cancellation possible. To overcome this problem the acquisition system is controlled by a digital signal processor (DSP) and thus the reaction time to a trigger is limited by how fast the DSP can respond. With this system the time variation between a trigger being received and the system starting a conversion is less than ± 0.1 μs which does not impact upon the cancellation performance.

8. Implementation of the active noise control system

Active noise control was implemented as an addition to the sound system described earlier. A Knowles EK3024 microphone was placed between the electrostatic diaphragm and the subject's ear mounted on the protective plastic grid of the headphones (see Fig. 2). The position of the microphone was important to achieve good subjective cancellation and several positions were evaluated. Directly opposite the entrance to the ear canal produced the best results. Tests in an MRI scanner showed that the Knowles microphone, although tiny, created distortion in the MRI image and, if too close to the subject's head, this distortion proved to be unacceptably large. The microphone required a copper screened lead to connect it to the active noise control system, which also introduced RFI and image distortion. This was minimised, but not eliminated, by keeping it as far away from the head as possible. However, the full solution to this problem was the substitution of the Knowles microphone with an optical microphone (see below). The active noise control unit was housed in a separate box connected to the microphone outputs and providing an audio cancellation output that was mixed with the stimulus required and fed to the headphone amplifier.

9. Operation of the active noise control system

The subject places the noise control headphones on their head and lies on the patient bed. Once in the scanner bore the plant models are obtained from the left and right ears. Using MLS click trains these take no more than 2 s per side. The active noise control unit is switched into record mode and the scanner is run for one fMRI volume acquisition. Recording is started on receipt of a trigger and lasts for a predetermined length of time sufficient to capture the full volume acquisition sound. The noise control unit is then switched to control mode and the scanner is operated as usual.

10. Active noise control performance

Recording noise-control systems were implemented independently in each side of our MRI sound system.

10.1. Objective performance measurements

While the system was designed specifically for a scanner that produced a sound with fundamental frequency of 1.9 kHz, we evaluated its general utility by simulating a range of possible scanner frequencies and measuring the attenuation of each fundamental frequency component that the system could achieve as measured at the error microphone.

We first made an accurate estimate of the spectrum of the real scanner sound (fundamental frequency 1.9 kHz; see Fig. 1) by capturing a sequence of the sounds and averaging their spectra obtained by fast Fourier transformation. The spectral amplitude values were then scaled to produce seven further spectra with fundamental frequencies of 500, 750, 1000, 1500, 2000, 2500, 3000, and 3500 Hz. These amplitude coefficients were used to program minimum phase finite impulse response filters which in turn were used to filter a 7-ms burst of white noise. This resulted in sounds with the same spectral shape as the original scanner sound but with the spectrum shifted up or down in frequency. Sixteen of these filtered noises were concatenated (to simulate a typical volume acquisition sequence) and reverberated using a simulation of a moderately echoic room. The resulting stimuli sounded subjectively like the noise within the bore of a scanner sampling a 16-slice volume during with echo-planar-imaging.

The simulated scanner noises and two real scanner noises (1.5 kHz and 0.65 kHz fundamental frequencies) were presented through speakers mounted in a simulated head coil within a wooden bore to simulate the acoustic environment of a scanner. Signals were captured from the error microphone inside the headset with and without active noise control and differences between the spectra were calculated.

The attenuation of the fundamental frequency component as a function of its frequency is shown in Fig. 6B with the black dots representing simulated scanner sounds and the

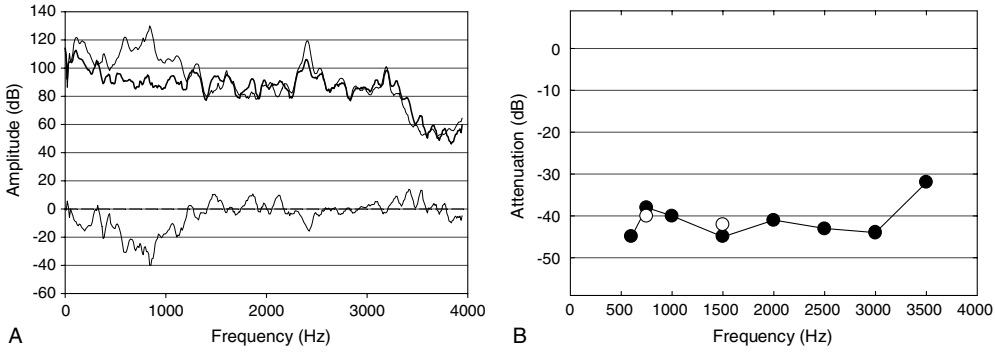

Fig. 6. (A) The spectra obtained from the error microphone both without (thin line) and with active noise control (thick line). The thin line at the bottom is the difference between the with and without values. (B) The difference between the spectra at the fundamental frequencies of simulated and recorded scanner sounds as a function of frequency (from [24] with permission).

white dots representing recorded scanner sounds. From 0.6 to 3 kHz approximately 40 dB of attenuation was achieved falling to 30 dB at 3.5 kHz. The attenuation of the simulated and real sounds is similar leading us to believe that our simulated sounds are accurate. Thus the recording noise-control system achieves appreciable objective noise reduction across a wide frequency range. The system was designed to operate only up to 4 kHz and includes anti-alias filters that cut in at 3800 Hz, possibly contributing to the reduced attenuation at 3500 Hz. Fig. 6A shows the uncancelled (thin line) and cancelled (thick line) spectra together with the difference (bottom line) as measured at the error microphone for a scanner sound with a fundamental frequency of 900 Hz. For more details see Chambers et al. [24].

10.2. Subjective performance measurements

Subjective benefits of the stereo noise control system were evaluated by loudness matching measurements: listeners listened to recorded scanner sounds with and without active noise control and adjusted the level of an independent sound to match the loudness of the scanner sounds. The scanner sounds were digital recordings made within the bores of two different 3 T scanners during EPI (see [1]) and consisted of harmonic complex tones with fundamental frequencies of 600 Hz and 1900 Hz (as shown in Fig. 1).

The matching stimuli were versions of the same scanner sounds, filtered to remove energy at frequencies remote from the fundamental since the active noise control mainly attenuates components in that range. Subjects therefore matched the loudness of the component that was most affected by noise reduction.

The scanner sounds were presented to the subjects in a simulated MRI scanner (see [24]) at 85 dB SPL and 95 dB SPL (as measured at the center of the "head coil", with the listener absent). Cancellation signals were generated for each ear separately and matching stimuli (binaurally) were presented through the MRI sound system. The scanner sound was presented and followed after an 800-ms silent interval by the corresponding matching stimulus. Loudness matching was performed using a one-up, one-down adaptive procedure [25]. The difference between the levels of the matching stimuli in the noise-reduction and control conditions was taken as a measure of the subjective noise reduction.

Four normal hearing listeners with extensive experience in psychoacoustic tasks participated. Each listener matched each of the eight conditions twice (two fundamental frequencies by two intensity levels, each with the controller on and off) and the two values of subjective noise reduction for each condition were averaged. The ordering of the conditions was random and was different for each listener.

The matching sound level in the control conditions was 8.5 dB (95% confidence interval 6.8–10.3) higher for scanner sounds at 95 dB SPL than at 85 dB SPL, (range 6.0–12.8 dB). This is not significantly different from the 10-dB difference in the stimuli and suggests that the loudness matching measures are reasonably accurate. Fig. 7 shows the subjective scanner noise reduction as the difference in the level of the matching stimulus between the noise-reduction and the control conditions for individual subjects. The matching sound was always less in the noise-reduction condition than in the control condition. This subjective benefit averaged 12 dB at 600 Hz and 5 dB at 1900 Hz. Thus at least for prerecorded scanner sounds in a simulated scanner environment the active noise control can achieve useful subjective attenuation at both 600 and 1900 Hz.

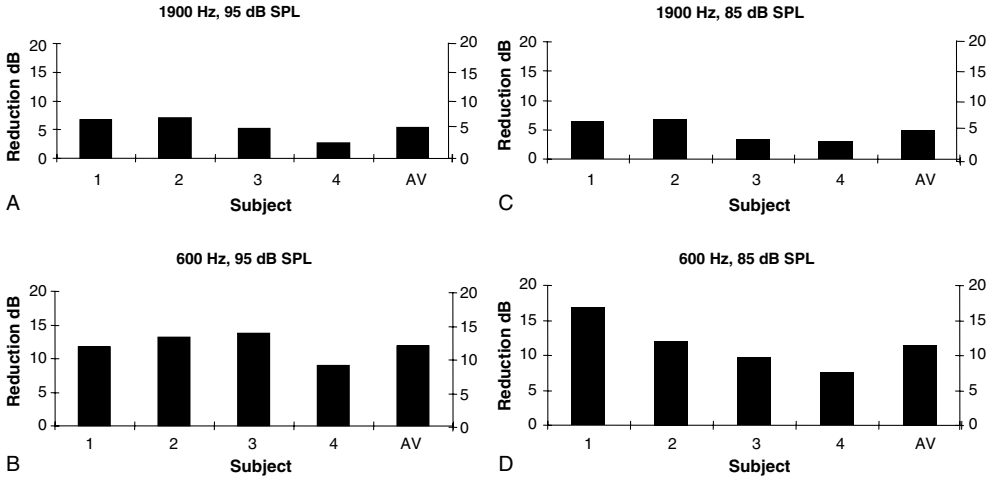

Fig. 7. Subjective reduction of the scanner sounds at two sound levels and two fundamental frequencies (as indicated) for four subjects. AV average of the four subjects (from [24] with permission).

11. Further technical developments

11.1. Optical acoustic transducers

A major problem, as we described earlier, with any equipment to be used in MRI scanners is their metallic content and their electrical signals that breach the scanner screening, leading to magnetic susceptibility and interference that degrades the images. While careful design in our present system has reduced many of these problems, a more radical approach detailed here has the potential of removing these problems completely by using fully optically driven headphones and microphones. To investigate this possibility we have been working with Phone-Or Ltd. who have developed and patented such technology. For full details on the design of the opto-acoustical headset, see Kahana et al. [26].

11.2. The fibre optic microphone

The principles of Phone-Or's optical microphones are described in detail in patents, and in various publications [27–32]. The construction of the intensity modulated optical microphone is depicted in Fig. 8A. The 'reflecting sensor' consists of a light emitting diode (LED) to provide a source of light (1), and a photodiode or a phototransistor to act as the photo-detector (2). Light from the LED (1) passes along the optic fibre (3,6) to illuminate a MEMS (micro-electro-mechanical-systems) membrane that includes a reflecting spot (8). Light reflected back from the spot passes through the second optic fibre (4,7) to the photo-detector (2) and to the measuring collecting unit (10). The movement of the membrane, and its reflecting spot, results in a change in the light intensity detected by the photo-detector (2) and hence to an electrical audio signal. The components of the optical microphone are presented in Fig. 8B, where the microphone head and fibres are non-metallic, and so do not affect the scanner images. They are also unaffected by the magnetic and electro-magnetic fields of the scanner.

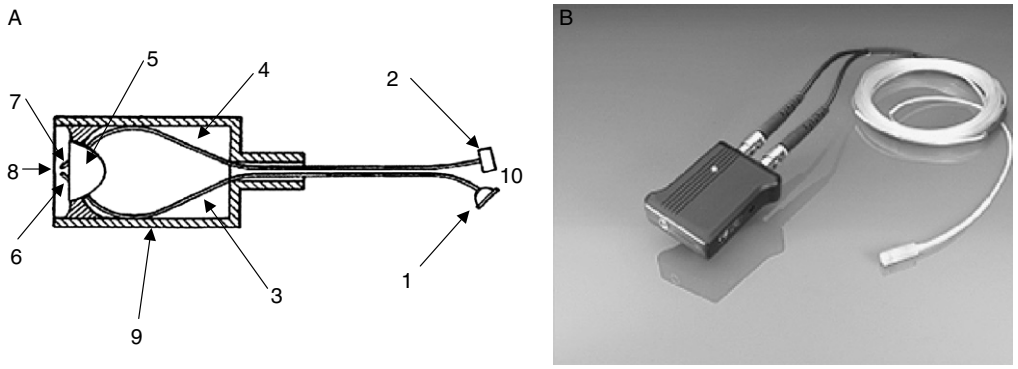

Fig. 8. (A) Schematic drawing of the basic construction of a modulated light intensity optical microphone (see sub-components description in the text). (B) A picture of the microphone comprising the optical head and the sensor itself, optical fibres, and the electro-optic unit which is positioned in a remote location (from [27] with permission).

The transduction process consists of three stages: mechanical (membrane displacement), optical (light modulation), and finally electrical (electrical signal modulation). The first two stages are take place in the scanner with the final stage in the control room, thus leaving a completely passive microphone inside the scanner room.

In collaboration with Phone-Or Ltd., we have replaced the Knowles error microphones in our active noise control systems with the optical microphones, confirmed that they cause no susceptibility or interference problems, and have achieved the same levels of active noise control with them.

11.3. Light-powered speakers

Generation of sound from the light-powered speaker (so called 'OptiSpeaker') requires three stages: (1) electro-optical (conversion of analogue voltage to modulated light), (2) opto-electrical (conversion of light to analogue voltage) and (3) electro-mechanical (conversion of analogue voltage to membrane displacement – sound). The first can take place in the MRI control room, but the other two must be in the scanner room.

Assuming the maximum peak sound levels in an EPI scan is 120–130 dB SPL, the ear defenders should reduce this to 100–110 dB SPL, therefore for such a transducer to be useable for active noise control it needs to be capable of such high levels of output with a bandwidth of at least 100–3500 Hz. There are two main objectives in the design of such a transducer: (1) optimising acoustical performance to this specific task; (2) minimising dimensions and electrical interference.

To date we have checked that prototype versions of the optically powered loudspeakers cause no interference or susceptibility problems in the scanner. In addition, objective measurements were undertaken in the same MRI acoustic simulator used before, with our original electrostatic headset (see results presented in Fig. 6A). Fig. 9A and B shows the pressure detected at the optical microphone with (the thick lines) and without ANC (the thin lines) in the time and frequency domain, respectively, using the Opti-Speaker in the headset. It can be seen that the main resonance at

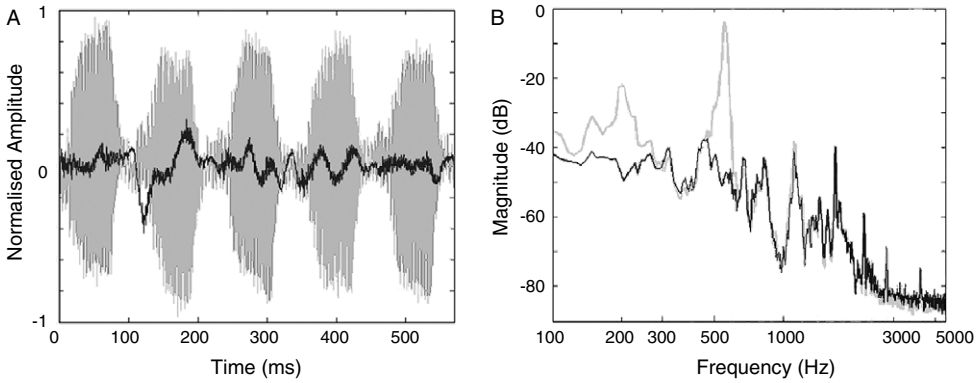

Fig. 9. Wave forms, in (A), and their spectra, in (B), with similar setup used with the original headset at the scanner replica at SPL = 114 dB. Noise reduction level of the fundamental resonance frequency is shown at 560 Hz (44 dB). Another resonance appears at 200 Hz and the system attenuates it by 28 dB.

600 Hz is attenuated by approximately 44 dB, and also sound energy at a frequency of around 200 Hz is attenuated by approximately by 28 dB.

11.4. Possible method of reducing the bone conducted sound reaching the subjects' inner ear

In principle, addition of the passive ear defender attenuations (Fig. 3) to those we measure resulting from the active noise control (Fig. 6) should achieve levels of up to 80 dB. In practice the benefit to the subjects is considerably less than this reaching only 10–50 dB (adding the passive (Fig. 3) and subjective benefits (Fig. 7)). The reason for the discrepancy between the objective reduction in airborne sound and the subjective benefit is almost certainly due to bone conduction [15–18].

While the main acoustic input to the cochlea is airborne sound, via the outer and middle ears, it also receives sound directly from the vibrations of bones and tissues. The efficiency of this path into the cochlea is frequency dependant, but bone conduction is approximately 40–60 dB [18] less sensitive than the acoustic path and normally does not play a material part in hearing. However, when the airborne sound at the ear is attenuated by more than 40 dB the bone conduction path becomes significant and may dominate the perceived sound. The total effective attenuation of our sound system at 650 Hz and 1900 Hz and hence the bone conduction limits (see [18]), can be obtained by adding the subjective benefits at these frequencies to the passive attenuation values. Further sound reduction of the airborne sound at the ear produces no subjective reduction of the perceived sound as the bone conduction path is dominant. Several groups have proposed ways to reduce this bone conduction imposed limit, mainly by reducing the sound levels impinging on the head and body with sound attenuating coverings. Wet suits, helmets and body coffins have all been proposed to try and reduce the sound that is impinging on the body (e.g. [15]). These have the obvious disadvantages that they are bulky, uncomfortable and some have safety issues, such as overheating of the subject.

If the bone conduction route to the cochlea is stable, there may possibly be way to reduce its effect. Subjects in the MRI scanner have reported that the residual sound

experienced is of constant amplitude thereby suggesting that the bone conduction path to the cochlea is stable. Békésy [33] demonstrated that the cochlea linearly mixes airborne and bone conducted sound by canceling a tone presented through headphones with a second tone presented through a bone vibrator. In principle therefore, it should be possible to cancel the bone vibration signal with an suitable airborne sound. The problem is estimating the amplitude and phase of the required airborne sound to cancel bone conducted sound generated by the MRI scanner. Given that the bone conduction operates directly on the cochlea it is not possible to measure this directly. It might however, be possible to estimate these parameters subjectively for each individual subject given that the main component of scanner noise is at a fairly narrow frequency band. The subject would have to adjust frequency, amplitude and phase of a continuous sine wave sound presented over the noise control system to reduce the residual bone conducted component of the subjective sound. Adding an extra path to the mixer (as shown by the dotted lines in Fig. 5) should then allow cancellation of the bone and airborne sound. If by such means, it is possible to produce material improvements in the subjective attenuation, it would be crucial to find out whether minor changes to the subject's position affected the bone conduction or whether it remains relatively stable.

References

[1] Foster JR, Hall DH, Summerfield AQ, Palmer AR, Bowtell RW. Sound level measurements and calculations of safe noise dosage during EPI at 3 T. J Mag Reson Imag 2000;12:157–63.
[2] Scarff CJ, Dort J, Eggermont JJ, Goodyear BJ. The effect of MR scanner noise on auditory cortex activity using fMRI. Human Brain Map 2004;22(4):341–9.
[3] Moelker A, Pattyinama PMT. Acoustic noise concerns in functional magnetic resonance imaging. Human Brain Map 2003;20:123–41.
[4] Yetkin FZ, Roland PS, Purdy PD, Christensen WF. Evaluation of auditory cortex activation by using silent FMRI. Am J Otolaryngol 2003;24(5):281–9.
[5] Sharma G, Knox KT. Influence of resolution on scanner noise perceptibility. In: Image processing, image quality, image capture, systems conference; 2001.
[6] Amaro E, Williams SCR, Shergill SS, Fu CHY, MacSweeney M, Picchioni MM, et al. Acoustic noise and functional magnetic resonance imaging: current strategies and future prospects. J Mag Reson Imag 2002;16(5):497–510.
[7] Mathiak K, Rapp A, Kircher TTJ, Grodd W, Hertrich I, Weiskopf N, et al. Mismatch responses to randomized gradient switching noise as reflected by fMRI and whole-head magnetoencephalography. Human Brain Map 2002;16(3):190–5.
[8] Mazard A, Mazoyer B, Etard O, Tzourio-Mazoyer N, Kosslyn SM, Mellet E. Impact of fMRI acoustic noise on the functional anatomy of visual mental imagery. J Cognit Neurosci 2002;14(2):172–86.
[9] Loenneker T, Hennel F, Ludwig Uea. Silent BOLD imaging. Mag Reson Mater Phys Biol Med 2001;13(2):76–81.
[10] Novitski N, Alho K, Korzyukov O, Carlson S, Martinkauppi S, Escera C, et al. Effects of acoustic gradient noise from functional magnetic resonance imaging on auditory processing as reflected by event-related brain potentials. NeuroImage 2001;14(1):244–51.
[11] Di Salle F, Formisano E, Seifritz E, Linden DEJ, Scheffler K, Saulino C, et al. Functional fields in human auditory cortex revealed by time-resolved fMRI without interference of EPI noise. NeuroImage 2001;13(2):328–38.
[12] Yang YH, Engelien A, Engelien W, Xu S, Stern E, Silbersweig DA. A silent event-related functional MRI technique for brain activation studies without interference of scanner acoustic noise. Mag Reson Med 2000;43(2):185–90.
[13] Hall DA, Haggard MP, Akeroyd MA, Palmer AR, Summerfield AQ, Elliott MR, et al. "Sparse" temporal sampling in auditory fMRI. Human Brain Map 1999;7(3):213–23.

[14] Hall DA, Haggard MP, Summerfield AQ, Akeroyd MA, Palmer AR, Bowtell RW. Functional magnetic resonance imaging measurements of sound-level encoding in the absence of background scanner noise. J Acoust Soc Am 2001;109(4):1559–70.
[15] Ravicz ME, Melcher JR. Isolating the auditory system from acoustic noise during functional magnetic resonance imaging: examination of noise conduction through the ear canal, head, and body. J Acoust Soc Am 2001;109:216–31.
[16] Berger EH. Laboratory attenuation of earmuffs and earplugs, both singly and in combination. Am Ind Hygiene Assoc J 1983;44:321–9.
[17] Berger EH. Method of measuring the attenuation of hearing protection devices. J Acoust Soc Am 1986;79:1655–87.
[18] Berger EH. Hearing protection: surpassing the limits to attenuation imposed by the bone conduction pathways. J Acoust Soc Am 2003;114:1955–67.
[19] Nelson PA, Elliot SJ. Active control of sound. San Diego, CA: Academic Press; 1992.
[20] Widrow B, Hoff ME. Adaptive switching circuits. IRE Western Electric Show Convention Record 1960;Part 4:96–104.
[21] Widrow B, Stearns SD. Adaptive signal processing. Englewood Cliffs, NJ: Prentice-Hall; 1985.
[22] Davies WDT. Generation and properties of maximum length sequences. Control 1966:364–5.
[23] Thornton ARD. MLS and Volterra Series in the analysis of transient evoked Oto-acoustic emissions. Brit J Audiol 1997;31:493–8.
[24] Chambers J, Akeroyd MA, Summerfield AQ, Palmer AR. Active control of the volume acquisition noise in functional magnetic resonance imaging: method and psychoacoustical evaluation. J Acoust Soc Am 2001;110(6):3041–54.
[25] Levitt H. Transformed up–down methods in psychoacoustics. J Acoust Soc Am 1971;49:467–77.
[26] Kahana Y, Kots A, Mican S, Chambers J, Bullock D. Optoacoustical ear defenders with active noise reduction in an MRI communication system. In: Active 2004, Williamsburg, VA; 2004.
[27] Kahana Y, Paritsky A, Kots A, Mican S. Recent advances in optical microphone technology. In: 32nd International congress and exposition on noise control engineering. Korea: Internoise; 2003.
[28] Paritsky A, Kots A. Sensor and method for measuring distance to, and/or physical properties of, a medium; 2002.
[29] Paritsky A, Kots A. Fiber optic distance sensor with sub-angstrom resolution. In: SPIE – The International Society for Optical Engineering, Boston, MA; 1999.
[30] Kots A, Paritsky A. Fiber optic microphone for harsh environment. In: SPIE – The International Society for Optical Engineering, Boston, MA; 1999.
[31] Paritsky A, Kots A. Optical microphone's break-through. In: 107th AES, New York; 1999.
[32] Bilaniuk N. Optical microphone transduction techniques. Appl Acoust 1997;50:35–63.
[33] Bekesy G. Experiments in hearing. New York: McGraw-Hill; 1960.